

Article

Comparison of a Nanofiber-Reinforced Composite with Different Types of Composite Resins

Zümür Ceren Özdoğan¹, Burcu Oglakci^{1,*}, Derya Merve Halacoglu Bagis², Binnur Aydoğan Temel³
and Evrim Eliguzeloglu Dalkilic¹

¹ Department of Restorative Dentistry, Faculty of Dentistry, Bezmialem Vakif University, 34093 Istanbul, Turkey; zumrutcerenozduman@gmail.com or zozduman@bezmialem.edu.tr (Z.C.Ö.)

² Private Clinic, Çekmeköy, 34794 Istanbul, Turkey; mrvhal@yahoo.com

³ Department of Pharmaceutical Chemistry, Faculty of Pharmacy, Bezmialem Vakif University, 34093 Istanbul, Turkey

* Correspondence: burcu923@hotmail.com or boglakci@bezmialem.edu.tr; Tel.: +90-(212)453-1850

Abstract: The aim of this study was a comprehensive evaluation and comparison of the physical and mechanical properties of a newly developed nano-sized hydroxyapatite fiber-reinforced composite with other fiber-reinforced and particle-filled composites. Commercially available eight composite resins (3 fiber-reinforced and 5 particle-filled) were used: Fiber-reinforced composites: (1) NovaPro Fill (Nanova): newly developed nano-sized hydroxyapatite fiber-reinforced composite (nHAFC-NF); (2) Alert (Pentron): micrometer-scale glass fiber-reinforced composite (μ mGFC-AL); (3) Ever X Posterior (GC Corp): millimeter-scale glass fiber-reinforced composite (mmGFC-EX); Particle-filled composites: (4) SDR Plus (Dentsply) low-viscosity bulk-fill (LVBF-SDR); (5) Estelite Bulk Fill (Tokuyama Corp.) low-viscosity bulk-fill (LVBF-EBF); (6) Filtek Bulk Fill Flow (3M ESPE) low-viscosity bulk-fill (LVBF-FBFF); (7) Filtek Bulk Fill (3M ESPE) high-viscosity bulk-fill (HVBF-FBF); and (8) Filtek Z250 (3M ESPE): microhybrid composite (μ H-FZ). For Vickers microhardness, cylindrical-shaped specimens (diameter: 4 mm, height: 2 mm) were fabricated ($n = 10$). For the three-point bending test, bar-shaped ($2 \times 2 \times 25$ mm) specimens were fabricated ($n = 10$). Flexural strength and modulus elasticity were calculated. AcuVol, a video image device, was used for volumetric polymerization shrinkage (VPS) evaluations ($n = 6$). The polymerization degree of conversion (DC) was measured on the top and bottom surfaces with Fourier Transform Near-Infrared Spectroscopy (FTIR; $n = 5$). The data were statistically analyzed using one-way ANOVA, Tukey HSD, Welsch ANOVA, and Games–Howell tests ($p < 0.05$). Pearson coefficient correlation was used to determine the linear correlation. Group μ H-FZ displayed the highest microhardness, flexural strength, and modulus elasticity, while Group HVBF-FBF exhibited significantly lower VPS than other composites. When comparing the fiber-reinforced composites, Group mmGFC-EX showed significantly higher microhardness, flexural strength, modulus elasticity, and lower VPS than Group nHAFC-NF but similar DC. A strong correlation was determined between microhardness, VPS and inorganic filler by wt% and vol% ($r = 0.572$ – 0.877). Fiber type and length could affect the physical and mechanical properties of fibers containing composite resins.

Keywords: composite; fiber; polymer; nano; mechanical; physical properties



Citation: Özdoğan, Z.C.; Oglakci, B.; Halacoglu Bagis, D.M.; Aydoğan Temel, B.; Eliguzeloglu Dalkilic, E. Comparison of a Nanofiber-Reinforced Composite with Different Types of Composite Resins. *Polymers* **2023**, *15*, 3628. <https://doi.org/10.3390/polym15173628>

Academic Editor: Gaetano Paolone

Received: 25 July 2023

Revised: 26 August 2023

Accepted: 27 August 2023

Published: 1 September 2023



Copyright: © 2023 by the authors. Licensee MDPI, Basel, Switzerland. This article is an open access article distributed under the terms and conditions of the Creative Commons Attribution (CC BY) license (<https://creativecommons.org/licenses/by/4.0/>).

1. Introduction

Composite resins find extensive application as restorative materials in contemporary dentistry. Clinical lifespan of composite resin restorations can vary due to factors related to the tooth, risks associated with the patient, chosen restorative techniques, and the materials implemented [1]. Adverse outcomes, such as marginal mismatch, marginal discoloration, microleakage, recurrent caries, and postoperative sensitivity, encountered in composite resin restorations are typically attributed to polymerization shrinkage. Studies have found

that the volumetric shrinkage of composite resins ranges from 1% to 6% [2]. Another common problem is fractures in composite resins applied to deep, large cavities. When subjected to stress, these fractures can be attributed to various mechanical properties of the composite resin, including fracture strength, elasticity, and marginal degradation. These factors can be assessed through tests, such as flexural properties and fracture strength [3].

The filler amount and types, organic monomers (e.g., Bis-GMA and TEGDMA) inorganic and organic matrix interfaces can affect the mechanical and physical properties [4–6]. The mechanical characteristics of composites can be improved to withstand chewing stresses by modifying the filler particle size and morphology. This modification has been shown to improve their overall performance. Regarding the type of filler used, composites can be categorized into fiber-reinforced and particle-filled composites [7,8]. Fibers are crucial for reinforcing composites by acting primarily as crack stoppers, thus enhancing mechanical properties that closely resemble those of natural tissues. The effectiveness of fiber-reinforced composite resins is significantly influenced by microstructural properties, including fiber loading, fiber orientation, fiber diameter, fiber length, and the adhesion between fibers and the polymer matrix. These composite resins strengthen teeth and mimic dentin's stress-absorbing characteristics, making them suitable for direct restoration of extensive cavities in vital and devital posterior teeth [9].

Several manufacturers have produced short fiber-reinforced composites (SFRCs) to address the limitations of conventional composite resins. These SFRCs attempt to structurally resemble the fibrous composition of dentin, and some are specifically recommended for bulk bases in high-stress-bearing areas. According to fiber aspect ratio theory, these materials can be classified as either high aspect ratio SFRCs with short fiber lengths on a millimeter scale or low aspect ratio SFRCs with short fiber lengths on a micrometer scale. One of the commercial forms of high aspect ratio SFRC is EverX Posterior (GC Corp., Tokyo, Japan), which consists of polyethylene and glass fibers, in millimeters (mm) scale. Low aspect ratio SFRC is Alert (Pentron, Wallingford, CT, USA), which is a dimethacrylate-based material with glass fibers in micrometer (μm) scale [10]. A new fiber-containing composite launched in 2018 has been added to composites reinforced with calcium-phosphate (hydroxyapatite). NovaPro Fill (Novova, MO, USA) is noteworthy for being the first composite to incorporate fiber filler material with dimensions that are measured in nanometers, representing an innovation on the nano-scale [11].

Microhybrid composites are frequently preferred as particle-filled composite resins in the posterior region due to high wear resistance. Recently launched bulk-fill composites also belong to the particle-filled composite class, and many brands produce them using different technologies. Different types of bulk-fill composite resins can be classified according to their viscosity: flowable (low-viscosity) and sculptable (high-viscosity) bulk-fill composites. The viscosity of bulk-fill composites is influenced by factors such as the type and quantity of fillers used in the composite as well as the content of the organic matrix. Bulk-fill composites have been launched on the market with claims of polymerizing in thicker layers (4–5 mm), showing lower polymerization shrinkage, and possessing physical properties that improved upon conventional composite resins [12,13].

Limited data can be found in the literature comparing the properties of newly developed hydroxyapatite nanofiber-reinforced composites to different types of composite resins. Thus, in this study, a total of 8 commercial composite materials were utilized, categorized into 2 distinct composite groups: particle-filled and fiber-reinforced. The particle-filled composites were further divided into 2 subgroups: bulk-fill and microhybrid composites. As for the fiber-reinforced composites employed in this research, they were classified into 3 subgroups: nanometer, micrometer, and millimeter categories. The aim of the present study was a comprehensive evaluation and comparison of the physical and mechanical properties of a newly developed nano-sized hydroxyapatite fiber-reinforced composite with other fiber-reinforced composites (micrometer- and millimeter-scale fiber-reinforced) and particle-filled composites (low-viscosity and high-viscosity bulk-fill and microhybrid composites) used in the posterior region.

The null hypothesis of this in vitro study was as follows:

There would be no differences in microhardness, flexural strength, modulus elasticity, volumetric polymerization shrinkage, or degree of conversion between nanofiber-reinforced composite and other fiber-reinforced or particle-filled composites.

2. Materials and Methods

2.1. Sample Size Calculation

G * power 3.1 program was used for the purpose of sample size calculation based on the estimated effect size between groups. In this study, for each group, a minimum of 5 specimens were necessary to obtain a medium effect size ($d = 0.50$, 80% power, 5% type 1 error rate).

The composite resins used in this study, group names and their compositions are shown in Table 1.

Table 1. Composite resins used in this study and their compositions.

	Classification	Brand Name	Manufacturer	Filler Particle	Filler %	Organic Matrix
Fiber-reinforced composites	Nano-sized hydroxyapatite fiber-reinforced Composite	NovaPro Fill (nHAFC-NF) (A2 Shade) Lot No.: 050035	(Nanova, MO, USA)	Barium silicate glass, amorphous fumed silica, hydroxyapatite fiber (diameter in nanometer scale (50–200 nm) and length in range between 100 and 150 μm)	77 wt%, NA	Bis-EMA, UDMA, TEGDMA
	Micrometer-Scale Glass Fiber-Reinforced Composite	Alert ($\mu\text{mGFC-AL}$) (A2 Shade) Lot: 7015315	(Pentron, CT, USA)	Silica and micrometer scale length glass fiber (20–60 μm) and diameter of 6–10 μm	84 wt%, 62 vol%	Bis-GMA, UDMA, TEGDMA, THFMA
	Millimeter-Scale Glass Fiber-Reinforced Composite	EverX Posterior (mmGFC-EX) (Universal Shade) Lot: 1904183	(GC Corp., Tokyo, Japan)	Millimetre scale length glass fiber filler, Barium glass	76 wt%, 57 vol%	Bis-GMA, PMMA, TEGDMA
Particle-filled composites	Low-Viscosity Bulk-Fill Composite	SDR Plus Bulk Fill (LVBF-SDR) (A2 Shade) Lot: 2/2306000334	(Dentsply, DE, USA)	Silanated barium-alumino-fluoro-borosilicate glass; silanated strontium alumino-fluoro-silicate glass; surface treated fume silicas; ytterbium fluoride; synthetic inorganic iron oxide pigments, and titanium dioxide.	70.5 wt%/47.4 vol%	Modified UDMA, TEGDMA, dimethacrylate, trimethacrylate resins
	Low-Viscosity Bulk-Fill Composite	Estelite Bulk Fill (LVBF-EBF) (A2 Shade) Lot: E699	(Tokuyama Corp., Tokyo, Japan)	Supranano spherical filler Silica, Zirconia, Ytterbium trifluoride Filler particle size 200 nm	70 wt%/56 vol%	Bis-GMA, Bis-MPEPP, TEGDMA,

Table 1. Cont.

	Classification	Brand Name	Manufacturer	Filler Particle	Filler %	Organic Matrix
Particle-filled composites	High-Viscosity Bulk-Fill Composite	Filtek Bulk Fill (HVBF-FBF) (A2 Shade) Lot: N979068	(3 M ESPE, MN, USA)	Nonaggregated silica filler (20 nm), nonaggregated zirconia filler (4–11 nm), aggregated zirconia/silica cluster filler (20 nm silica/4–11 nm zirconia), and an agglomerate ytterbium trifluoride filler (100 nm)	76.5 wt%/58.4 vol%	AFM, AUDMA, UDMA, DDDMA
	Low-Viscosity Bulk-Fill Composite	Filtek Bulk Fill Flow (LVBF-FBFF) (A2 Shade) Lot: N934595	(3 M ESPE, MN, USA)	The zirconia/silica particles [size range of 0.01–3.5 µm (The average particle size is 0.6 µm)] Ytterbium trifluoride (particle-size range of 0.1–5.0 µm)	64.5 wt%/42.5 vol%	TEGDMA, BisGMA, Bis-EMA, Procrilat and UDMA
	Microhybrid-filled composite	Filtek Z250 (Z250) (µH-FZ) (A2 Shade) Lot: N968746	(3 M ESPE, MN, USA)	Silica/Zirconia, cluster fillers Filler particle size of 0.01–3.5 µm (average 0.6 µm)	82 wt%, 60 vol%	TEGDMA, UDMA, Bis-EMA

Abbreviations: Bis-EMA, ethoxylated bisphenol A dimethacrylate; UDMA, urethane dimethacrylate; TEGDMA: triethylene glycol dimethacrylate; Bis-GMA, bisphenol A-diglycidyl dimethacrylate; THFMA, tetrahydrofurfuryl methacrylate; PMMA, Polimetil metakrilat; Bis-MEPP, bisphenol A ethoxylate dimethacrylate; AFN, addition fragmentation monomer; AUDMA, aromatic dimethacrylate; DDDMA, 1,12-dodecane dimethacrylate; Bis-EMA, ethoxylated bisphenol A glycol dimethacrylate, vol, volume; wt, weight.

A single operator prepared specimens according to the manufacturer's instructions during all analyses.

2.2. Microhardness Measurements

Cylindrical-shaped specimens (height: 2 mm, diameter: 4 mm) of each composite resin were prepared using Teflon molds ($n = 10$) (Figure 1). The specimens were sandwiched between two transparent mylar strips and glass slides to achieve a smooth, polymerized surface. The excess material was then removed by applying pressure using the glass slides. Subsequently, the specimens were subjected to light polymerization through the upper glass slide with a light-emitting diode light-curing unit (LED LCU; Valo, Ultradent, UT, USA, irradiance of 1000 mW/cm²) for 20s. Periodically during specimen fabrication, a radiometer (Bluephase Meter II, Ivoclar Vivadent, Schaan, Liechtenstein) was used to control the light intensity to ensure it remained at that level. A permanent marker was used to mark the bottom surfaces. The specimens were then placed in a dark vial containing distilled water at 37 °C for 24 h. A Vickers microhardness test was performed with an HMV Microhardness Tester (HMV-G, Shimadzu Corp., Kyoto, Japan) according to the ASTM E384-17 standard [14]. Three measurements were obtained on each sample's top and bottom surfaces (200 g load, 10 s dwell time). Vickers hardness values were recorded as the average of these measurements. The hardness value of the bottom surface was divided by the hardness value of the top surface to determine the hardness ratios (%), and these ratios were later converted into percentages.



Figure 1. A specimen prepared for microhardness test.

2.3. Flexural Strength and Modulus Elasticity Measurements

ISO 4049 guidelines were followed to prepare 10 bar-shaped specimens ($2 \times 2 \times 25$ mm) for each composite resin (Figure 2). A half-split stainless steel mold was utilized in the preparation process [15]. A single increment of composite resin was placed into the mold, and it was then covered on both sides using two transparent mylar strips, along with glass slides.



Figure 2. A specimen prepared for three-point bending test.

A universal testing machine (AGS-X, Shimadzu Corp., Kyoto, Japan) was used for the three-point bending test at a 1.0 mm/min crosshead speed until fracture (Figure 3). The span length for the test was set at 15 mm. Analysis software (Trapezium X, Shimadzu Corp., Kyoto, Japan) was used to record the load-deflection curves and calculate the flexural strength (FS) using Equation (1) [16]:

$$FS = 3F/L(2wt^2) \quad (1)$$

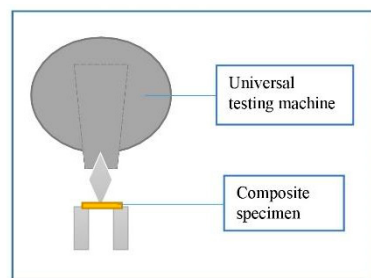


Figure 3. Schematic representation of three-point bending test.

Within this equation, “F” represents the maximum force, “L” denotes the distance between the supports, “w” signifies the width, and “t” indicates the thickness of the sample. The modulus elasticity (E) was determined by calculating the slope of the linear region in the load-deflection curve. This calculation was executed by dividing the load (F) by the displacement (d) in the linear elastic region. Equation (2) was used for this calculation.

$$E = (F/d)(L^3/[4wt^3]) \quad (2)$$

2.4. Volumetric Polymerization Shrinkage (VPS) Measurements by AcuVol Video Image Analysis

VPS was measured using a video image device (AcuVol, Bisco, Schaumburg, IL, USA) at 25 °C in single-view mode. Low-viscosity composites (LVBF-SDR, LVBF-EBF, and LVBF-FBFF) were syringed onto a 4.2-mm-diameter polytetrafluoroethylene (PTFE) pedestal, high-viscosity composites (μ H-FZ, nHAFC-NF, mmGFC-EX, μ mGFC-AL, and HVBF-FBF)

were rolled into a ball and placed on the PTFE pedestal in front of a CCD camera ($n = 6$). A resting period of five minutes was granted to the specimen to mitigate the impact of slumping on the measurement. The light-curing tip was fixed 1 mm above the top of the specimen and was then polymerized for 20 s with a LED LCU (1000 mW/cm^2). The volumetric shrinkage was measured five minutes after light polymerization to allow the specimen's temperature to stabilize at room temperature. Using the images taken before and after polymerization, the VPS rate was measured with this formulation and recorded as a percentage:

$$(V1-V2)/V1 \times 100 \quad (3)$$

Within this equation, "V1" represents the volume of the specimen before light polymerization; "V2" represents the volume of the specimen after light polymerization.

2.5. Degree of Conversion (DC) Measurements

Five specimens were prepared using cylindrical molds (height: 2 mm, diameter: 5 mm; $n = 5$) to determine the polymerization degree of conversion (DC) measurements. Each composite resin was placed into the molds and covered on both sides with two transparent mylar strips and glass slides to remove excess material and avoid oxygen inhibition. The light-curing tip was fixed on the top glass slide and the specimens were polymerized with an LED LCU (1000 mW/cm^2) for 20s. Periodically during specimen fabrication, a radiometer (Bluephase Meter II, Ivoclar Vivadent, Schaan, Liechtenstein) was used to control the light intensity to ensure it remained at that level. After light curing, they were kept at 100% humidity at 37°C for 24 h in a dark vial [11].

After polymerization, the degree of conversion (%) was calculated for the top and bottom surfaces with an attenuated total reflectance Fourier transform infrared spectrometer (ATR-FTIR; ALPHA Bruker spectrometer with a platinum-ATR accessory). Each composite resin was also measured by the ATR-FTIR before polymerization (Figure 4).

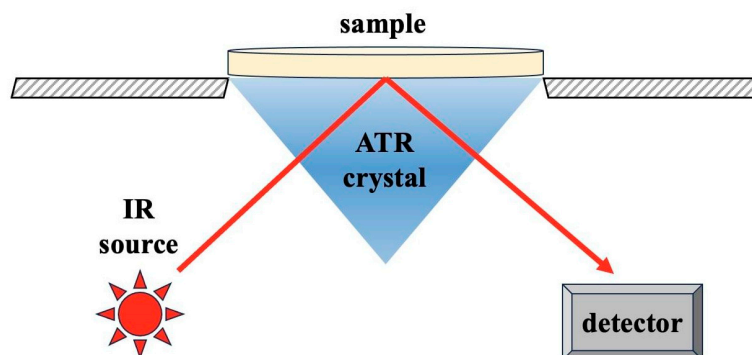


Figure 4. Schematic representation of attenuated total reflectance Fourier transform infrared spectrometer (ATR-FTIR) system.

The spectra were obtained using the following parameters to calculate the DC: a wave number range of $4000\text{--}600 \text{ cm}^{-1}$, 16 scans per spectrum, and a spectral resolution of 4 cm^{-1} . The stretching vibrations of the aliphatic $\text{C}=\text{C}$ bonds at 1636 cm^{-1} served as the analytical absorption band, while the aromatic $\text{C}=\text{C}$ bonds at 1607 cm^{-1} served as the internal reference absorption band. The DC value was determined by calculating the ratio of the peak heights of the analytical and reference absorption bands, which were then normalized by the ratio of the uncured monomers, as shown in the following equation:

$$DC\% = 1 - \left[\frac{\left(\frac{A_1}{A_2} \right)_{\text{polymer}}}{\left(\frac{A_1}{A_2} \right)_{\text{monomer}}} \right] \times 100 \quad (4)$$

This calculation is represented by the equation above, where A_1 and A_2 represent the peak intensities of the aliphatic $\text{C}=\text{C}$ (1636 cm^{-1}) and aromatic $\text{C}=\text{C}$ (1607 cm^{-1}) bonds, respectively. The subscripts outside the parentheses refer to the spectra before (monomer)

and after (polymer) light curing. The mean top and bottom DCs and standard deviations were determined for each type of material.

2.6. Statistical Analysis

A software program (SPSS 22.0 Windows, SPSS Inc., Chicago, IL, USA) was used. The Shapiro–Wilk and Levene’s tests determined the variables’ normality and the variances’ homogeneity for all data. Since the data were normally distributed but had heterogeneous variances for microhardness data, a Welsch’s ANOVA test was used to compare the materials. All pairwise comparisons were performed with the Games–Howell test. Since the data were normally distributed and had homogeneous variances for flexural strength, modulus elasticity, VPS, and DC values, a one-way analysis of variance (ANOVA) test was used to compare the materials. All pairwise comparisons were performed using the Tukey HSD test. Pearson coefficient correlation was performed to determine the linear correlation between microhardness, flexural strength, VPS and inorganic filler content. A significance level of 0.05 was considered for all analyses.

3. Results

3.1. Microhardness Measurements

The mean microhardness values (HV) and standard deviations of all groups are shown in Table 2.

Table 2. Mean microhardness values (HV) and standard deviations (\pm SD) of top and bottom surfaces for all groups; bottom/top microhardness ratio (%).

Groups	Top (HV)	Bottom (HV)	Bottom/Top (%)
nHAFC-NF	62.15 \pm 2.33 ^c	39.29 \pm 7.85 ^{ab}	63.21
μ mGFC-AL	72.67 \pm 3.39 ^d	45.53 \pm 5.50 ^b	62.65
mmGFC-EX	71.43 \pm 2.74 ^d	68.53 \pm 0.94 ^d	95.94
LVBF-SDR	37.04 \pm 2.27 ^a	33.22 \pm 2.67 ^a	88.82
LVBF-EBF	48.73 \pm 1.39 ^b	47.23 \pm 2.56 ^b	96.92
HVBF-FBF	69.08 \pm 3.22 ^d	61.30 \pm 3.44 ^c	88.73
LVBF-FBFF	35.73 \pm 1.00 ^a	34.17 \pm 1.10 ^a	95.63
μ H-FZ	96.54 \pm 2.07 ^e	87.12 \pm 2.48 ^e	90.24
<i>p</i>	<0.001	<0.001	

Different lower-case letters indicate the significant differences within the given column ($p < 0.05$).

On the top surfaces, compared to other groups, Group μ H-FZ showed the statistically highest HV. Comparing the fiber-reinforced composites, Group mmGFC-EX and Group μ mGFC-AL showed statistically higher microhardness than Group nHAFC-NF. Comparing the particle-filled composites, Group HVBF-FBF showed statistically higher HV than Group LVBF-FBFF, Group LVBF-SDR, and Group LVBF-EBF.

On the bottom surfaces, compared to other groups, Group μ H-FZ had the statistically highest HV. Comparing the fiber-reinforced composites, Group mmGFC-EX exhibited statistically higher HV than Group μ mGFC-AL and Group nHAFC-NF. Comparing the particle-filled composites, Group HVBF-FBF exhibited statistically higher HV than Group LVBF-FBFF, Group LVBF-SDR, and Group LVBF-EBF.

Group nHAFC-NF (63.21%) and Group μ mGFC-AL (62.65%) exhibited a lower hardness ratio than threshold values (80%). Other tested groups showed a hardness ratio exceeding the 80% threshold values.

3.2. Flexural Strength and Modulus Elasticity Measurements

The mean flexural strength (MPa), modulus elasticity (GPa) values, and standard deviations (\pm SD) of all the tested groups are shown in Table 3.

Table 3. The mean flexural strength, modulus elasticity and VPS values and standard deviations (\pm SD) for all groups.

Groups	Flexural Strength (MPa)	Modulus Elasticity (GPa)	VPS (%)
	Mean \pm SD	Mean \pm SD	Mean \pm SD
nHAFC-NF	134.32 \pm 25.09 ^{ab}	12.27 \pm 2.29 ^{ab}	3.33 \pm 0.19 ^{cd}
μ mGFC-AL	107.66 \pm 51.58 ^a	9.83 \pm 4.71 ^a	2.76 \pm 0.22 ^{bc}
mmGFC-EX	226.25 \pm 37.19 ^c	20.66 \pm 3.40 ^c	2.62 \pm 0.34 ^b
LVBF-SDR	140.61 \pm 26.13 ^{ab}	12.84 \pm 2.39 ^{ab}	4.12 \pm 0.46 ^{ef}
LVBF-EBF	138.09 \pm 23.66 ^{ab}	12.61 \pm 2.16 ^{ab}	3.73 \pm 0.45 ^{de}
HVBF-FBF	162.05 \pm 38.28 ^b	14.80 \pm 3.50 ^b	1.89 \pm 0.39 ^a
LVBF-FBFF	117.16 \pm 36.93 ^{ab}	10.70 \pm 3.37 ^{ab}	4.71 \pm 0.47 ^{fg}
μ H-FZ	259.26 \pm 42.99 ^c	23.68 \pm 3.93 ^c	2.72 \pm 0.12 ^{bc}
<i>p</i>	<0.001	<0.001	<0.001

Different lower-case letters indicate the significant differences within the given column ($p < 0.05$).

Compared to other groups, Group μ H-FZ and Group mmGFC-EX exhibited the statistically highest flexural strength and modulus elasticity. Comparing the fiber-reinforced composites, Group nHAFC-NF showed similar flexural strength and modulus elasticity to Group μ mGFC-AL. Comparing the particle-filled composites, Group HVBF-FBF exhibited similar flexural strength and modulus elasticity to Group LVBF-FBFF, Group LVBF-SDR, and Group LVBF-EBF.

3.3. VPS Measurement by AcuVol Video Image Analysis

The mean VPS (%) values and standard deviations (\pm SD) with the AcuVol video image analyzer for all groups are shown in Table 3.

Compared to other groups, Group HVBF-FBF showed the statistically lowest VPS. Comparing the fiber-reinforced composites, Group mmGFC-EX had a lower VPS than Group nHAFC-NF. Comparing the particle-filled composites, Group μ H-FZ had statistically lower VPS than Group LVBF-EBF, Group LVBF-FBFF, and Group LVBF-SDR.

3.4. DC Measurements

The DC values (%) and standard deviations (\pm SD) of all groups at the top and bottom surfaces are shown in Table 4.

Table 4. The mean DC values (%) and standard deviations (\pm SD) of all groups at the top and bottom surfaces.

Groups	Top	Bottom
nHAFC-NF	60.56 \pm 2.96 ^e	52.44 \pm 4.52 ^c
μ mGFC-AL	48.18 \pm 2.88 ^{ab}	43.26 \pm 2.17 ^{ab}
mmGFC-EX	56.18 \pm 2.32 ^{de}	49.56 \pm 4.01 ^{bc}
LVBF-SDR	46.66 \pm 3.38 ^a	40.22 \pm 3.34 ^a
LVBF-EBF	50.40 \pm 1.61 ^{abc}	45.38 \pm 3.38 ^{abc}
HVBF-FBF	55.00 \pm 4.05 ^{cde}	48.32 \pm 2.28 ^{bc}
LVBF-FBFF	53.62 \pm 2.11 ^{bcd}	47.32 \pm 4.96 ^{abc}
μ H-FZ	51.44 \pm 1.75 ^{abcd}	46.20 \pm 1.81 ^{abc}
<i>p</i>	<0.001	<0.001

Different lower-case letters indicate the significant differences within the given column ($p < 0.05$).

At the top and bottom, compared to other groups, Group LVBF-SDR had the lowest DC, and Group nHAFC-NF had the highest DC.

At the top, comparing the fiber-reinforced composites, Group mmGFC-EX showed statistically higher DC than Group μ mGFC-AL, while it showed a similar DC to Group nHAFC-NF. Comparing the particle-filled composites, Group μ mH-FZ exhibited a similar DC to Group LVBF-SDR, Group HVBF-FBF, Group LVBF-FBFF, and Group LVBF-EBF.

At the bottom, comparing the fiber-reinforced composites, Group mmGFC-EX had a similar DC to Group nHAFC-NF and Group μ GFC-AL, and Group nHAFC-NF had a statistically higher DC than Group μ GFC-AL. Comparing the particle-filled composites, Group μ H-FZ had a similar DC to Group LVBF-SDR, HVBF-FBF, LVBF-FBFF, and LVBF-EBF.

3.5. Linear Correlation between Physical and Mechanical Properties and Inorganic Filler Content

Linear correlation analysis for all groups comparing microhardness, flexural strength, VPS and filler content (wt/vol%) is shown in Table 5. A very strong correlation ($r = 0.841$ – 0.877) on the top and a moderate correlation ($r = 0.572$ – 0.668) on the bottom, were detected between microhardness and inorganic filler by wt% and vol%. A weak correlation ($r = 0.364$ – 0.385) was found between flexural strength and inorganic filler by wt% and vol%. A strong correlation ($r = 0.776$ – 0.860) was present between VPS and inorganic filler by wt% and vol%.

Table 5. Linear correlation analysis between microhardness, flexural strength, VPS and inorganic filler content (wt/vol%).

	Correlation Coefficient (r)	p
Filler %wt-microhardness bottom	0.572	0.139
Filler %wt-microhardness top	0.877	0.004
Filler %wt-flexural strength	0.364	0.375
Filler %wt-VPS	−0.776	0.023
Filler %vol-microhardness bottom	0.668	0.101
Filler %vol-microhardness top	0.841	0.018
Filler %vol-flexural strength	0.385	0.394
Filler %vol-VPS	−0.86	0.013

4. Discussion

Despite significant advancements in restorative composites, fiber-containing restorative materials still exhibit two primary limitations: inadequate mechanical strength and polymerization shrinkage. Several studies on nanofiber-reinforced composites have focused on the orientation and distribution of fibers. There has been growing interest in enhancing composites by incorporating nanofibers. Within the currently available literature, published studies concerning restorative composites reinforced with nanofibers are limited. In this research, comprehensive evaluation and comparison of the physical and mechanical properties of a newly developed nano-sized hydroxyapatite fiber-reinforced composite with other fiber-reinforced composites (micrometer- and millimeter-scale fiber-reinforced), and particle-filled (low-viscosity and high-viscosity bulk-fill and microhybrid) composites used in the posterior region, was performed. Based on the findings, the null hypothesis that there would be no differences in microhardness, flexural strength, modulus elasticity, volumetric polymerization shrinkage, or degree of conversion between nanofiber-reinforced composite and other fiber-reinforced or particle-filled composites, was rejected.

The surface hardness of composite resins in posterior stress-bearing areas is a crucial mechanical property influenced by the effectiveness of polymerization and bonding between monomers [17]. Various factors related to resin composites, such as the size, shape, and fraction of fillers in the inorganic phase, can influence hardness. Hardness typically increases with higher filler content. The specific composition and structure of the organic matrix also impact hardness [18]. The properties of dental composites are associated with the volume fraction of fillers incorporated within the resin and the effectiveness of the

silanization procedure used to connect the filler and matrix phases. Stress within the material is primarily transferred through interactions between hard particles [19].

In this study, the microhybrid composite (82% wt) showed significantly higher microhardness on the top and bottom surfaces than the other composites. High-viscosity bulk-fill (76.5% wt), also showed significantly higher microhardness than low-viscosity bulk-fill composites. These findings align with several studies [19–21] of higher filler loading. Pearson coefficient correlation confirmed the fact that a positive correlation was determined between microhardness and filler content. Moreover, when comparing the fiber-containing composites, millimeter-scale fiber-reinforced composites exhibited significantly higher microhardness than nano-sized hydroxyapatite fiber-reinforced composites. The millimeter-scale glass fiber-reinforced composite contained fibers with lengths ranging from 1 to 2 mm, surpassing the critical fiber length. Consequently, incorporating these short fibers into a resin matrix could significantly improve mechanical properties. Uyar et al. [22] showed that aligning nanofibers enhanced dental composites' mechanical properties. Thus, the lack of alignment of nanofibers may have contributed to lower microhardness values for nanofiber-reinforced composites. Hardness values of bottom/top surfaces generally can be used to measure the degree of polymerization. In the literature, it was indicated that an acceptable degree of polymerization is considered successful if the bottom hardness corresponds to a minimum of 80% of the hardness of the top surface [23]. However, in this study, a hardness ratio lower than 80% was found for nanofiber-reinforced composite and micrometer-scale glass fiber-reinforced composite.

Flexural strength measures a material's ability to withstand maximum stress, such as chewing loads before it fails. It functions as an indicator of the durability of a restorative material when subjected to stress. Modulus elasticity describes the stiffness of the material [24,25]. These flexural properties can be influenced by factors such as filler size, morphology, and the amount of filler in the restorative material. Increased filler content and smaller spherical-shaped fillers typically increase packing density and enhance mechanical properties. However, other notable factors, including stress transfer between the matrix and the filler particles and adhesion between these components, can also impact flexural strength [26].

In the present study, microhybrid and millimeter-scale glass fiber-reinforced composites demonstrated significantly higher flexural strength and modulus elasticity than the other composites. This finding is in line with Yancey et al. [11] who reported that nanofiber-reinforced composite showed significantly lower flexural strength and modulus elasticity than microhybrid composite. Lassila et al. indicated that nanofiber-reinforced composite showed significantly lower modulus elasticity than millimeter-scale glass fiber-reinforced composite [9]. Millimeter-scale glass fiber-reinforced composite, with its 76% wt filler load and inclusion of glass fibers inside the polymer matrix, exhibited superior flexural properties [10]. This finding aligns with previous research by Suzuki et al., who also noted the excellent flexural characteristics of millimeter-scale glass fiber-reinforced composite [27]. In the present study, nanofiber-reinforced composite displayed a flexural strength and modulus elasticity similar to micrometer-scale glass fiber-reinforced composite. The nanofiber-reinforced composite contains fibers with diameters in the nanometer scale (50–200 nm) and lengths ranging from 100 to 150 μm , while micrometer-scale glass fiber-reinforced composite has fibers with diameters of 7 μm whose length is in the micrometer scale (20–60 μm). Those fibers containing materials have properties that fall below the critical fiber length and the desired aspect ratio (the ratio between length and diameter) [28]. Researchers have also noted that specific fiber-to-polymer ratios and resin concentrations can cause a decrease in flexural properties. This decrease has been attributed to limitations in the bonding between the fibers and the resin matrix or incomplete resin infiltration, leading to voids that compromise the material's strength. Among the many parameters reinforcing the fibers' efficiency, the fibers' orientation is especially important [29].

To assess the VPS of composite resins, AcuVol was chosen as the preferred method for its ease of use and cost-effectiveness. VPS is considered an unfavorable side effect

of composite resins [30]. The composition of composite resin, including the types of organic monomers (e.g., Bis-GMA and TEGDMA) and the types and content of inorganic fillers, can impact VPS. TEGDMA, with its lower molecular weight and higher number of double bonds, tends to increase VPS more than Bis-GMA [31]. However, an increase in filler content or the presence of pre-polymerized filler particles can result in decreased VPS. These factors influence the extent of VPS in composite resins. According to the literature, VPS values for high-viscosity resin composites typically range from 1% to 3%, while low-viscosity composites may exhibit VPS values of up to 6% [32]. In the current study, the VPS of all tested composites fell within the range of approximately 1% to 5%, which is considered clinically acceptable. Notably, the high-viscosity bulk-fill composite demonstrated a significantly lower VPS than the other tested materials. High-viscosity bulk-fill composite resin includes UDMA (urethane dimethacrylate) and two innovative methacrylate monomers: aromatic urethane dimethacrylate (AUDMA) and addition-fragmentation monomer (AFM). The purpose of incorporating these monomers is to specifically target and minimize the VPS in the composite material. The mechanism of action of AUDMA and UDMA, a high molecular weight monomer, reduces the number of reactive groups. This reduction helps moderate the volumetric shrinkage and stiffness of the polymer matrix, which in turn contributes to the development of polymerization stress. By minimizing the reactivity of the monomers, AUDMA and UDMA can effectively mitigate the extent of volumetric shrinkage and the associated stress during polymerization [33]. The presence of AFM in high-viscosity bulk-fill composite can reduce polymerization shrinkage stress without negatively affecting the polymer's physical properties. A combination of AUDMA, UDMA, and AFM reduces polymerization shrinkage stress while maintaining the favorable physical properties of the polymer composite [34]. This finding could be attributed to this restorative material's AFM and AUDMA monomer.

In this study, the microhybrid composite (82% wt) showed significantly lower VPS than low-viscosity bulk-fill composites (LVBF-SDR 70.5% wt, LVBF-Filtek Bulk Fill Flow /64.5% wt, and LVBF-Estelite Bulk Fill/70% wt). The lower VPS values may be attributed to the higher filler composition of the microhybrid composite. Besides, the Pearson coefficient correlation indicated a strong correlation between VPS and inorganic filler content. The literature has indicated that fiber-reinforced restorative materials can also function as a stress-distributing, energy-absorbing mechanism for reducing VPS while strengthening mechanical properties [35–37]. Comparing the fiber-containing composites, millimeter-scale glass fiber-reinforced composite exhibited significantly lower VPS than nanofiber-reinforced composite.

The DC usually represents the degree of polymerization or the percentage of polymerizable double bonds converted to a single bond. The ideal composite resin material should have lower VPS and higher DC properties. Extensive documentation supports the notion that the high molecular weight Bis-GMA molecule, possessing a rigid aromatic backbone and robust intermolecular hydrogen-bonding capability, exhibits limited molecular mobility, reducing conversion within the polymer network [38]. Introducing the low-viscosity ethoxylated counterpart, known as Bis-EMA, as a partial replacement for Bis-GMA can enhance the crosslinking monomers' molecular reactivity [39]. Furthermore, the incorporation of low-molecular-weight TEGDMA and UDMA, recognized for their heightened mobility, contributes to an overall increase in the ultimate conversion process.

In this study, at the top and bottom, nanofiber-reinforced composite showed a similar DC to millimeter-scale glass fiber-reinforced composite while it exhibited significantly higher DC than micrometer-scale glass fiber-reinforced composite. The nanofiber-reinforced composite contains Bis-EMA, UDMA, TEGDMA, and no Bis-GMA, while millimeter-scale glass fiber-reinforced composite material consists of Bis-GMA, randomly distributed millimeter-scale length glass fibers and filler particles. The components of this material are expected to impede the penetration of activating light. However, in this study, one possible explanation for the observed higher DC values in millimeter-scale glass fiber-reinforced composite is the utilization of two photoinitiators, namely camphorquinone and

a derivative of trimethylbenzoylphosphine oxide. This combination produces more free radicals than camphorquinone alone, thus enhancing this material's DC [39]. The particle size of inorganic fillers can also significantly affect light scattering and, subsequently, DC properties. Xu et al. determined that the DC values of nanofiller resin composites were higher than those of microfiller resin composites [2]. Therefore, the nanofiber-reinforced composite's higher DC values could be explained by its filler particle size. Besides, the finding of this study is in line with Yancey et al., who reported that nanofiber-reinforced composite showed higher DC at the top and bottom than microhybrid composite [12].

5. Conclusions

In conclusion, A strong correlation was determined between microhardness, VPS and inorganic filler by wt% and vol%. Fiber type and length could affect fiber-containing composite resins' physical and mechanical properties. Microhybrid composite displayed the highest microhardness, flexural strength, and modulus elasticity, while high-viscosity bulk-fill exhibited significantly lower VPS than other composites. When comparing the fiber-containing composites, millimeter-scale glass fiber-reinforced composite showed significantly higher microhardness, flexural strength, modulus elasticity, and lower VPS than nanofiber-reinforced composite but similar DC.

Author Contributions: Conceptualization and design: Z.C.Ö., B.O., D.M.H.B., B.A.T. and E.E.D.; Literature review: Z.C.Ö., B.O., D.M.H.B., B.A.T. and E.E.D.; Formal analysis: Z.C.Ö., B.O., D.M.H.B., B.A.T. and E.E.D.; Investigation and data collection: Z.C.Ö., B.O., D.M.H.B., B.A.T. and E.E.D.; Data analysis and interpretation: Z.C.Ö., B.O., D.M.H.B., B.A.T. and E.E.D.; Writing: Z.C.Ö., B.O., D.M.H.B., B.A.T. and E.E.D.; Review & editing: Z.C.Ö., B.O., D.M.H.B., B.A.T. and E.E.D. All authors have read and agreed to the published version of the manuscript.

Funding: Bezmialem Vakif University Research Fund (Project No: 4.2019/22).

Institutional Review Board Statement: Not applicable.

Data Availability Statement: Not applicable.

Acknowledgments: This study was supported by the Bezmialem Vakif University Research Fund (Project No.: 4.2019/22). Many thanks to Assistant Professor Sevilay Karahan for her help with statistical analyses. The authors do not have any financial interest in the companies whose materials are included in this article.

Conflicts of Interest: The authors do not have any financial interest in the companies whose materials are included in this article.

References

1. Da Rosa Rodolpho, P.A.; Rodolfo, B.; Collares, K.; Correa, M.B.; Demarco, F.F.; Opdam, N.J.; Cenci, M.S.; Moraes, R.R. Clinical performance of posterior resin composite restorations after up to 33 years. *Dent. Mater.* **2022**, *38*, 680–688. [[CrossRef](#)]
2. Xu, T.; Li, X.; Wang, H.; Zheng, G.; Yu, G.; Wang, H.; Zhu, S. Polymerization shrinkage kinetics and degree of conversion of resin composites. *J. Oral Sci.* **2020**, *62*, 275–280. [[CrossRef](#)] [[PubMed](#)]
3. Garoushi, S.; Vallittu, P.K.; Watts, D.C.; Lassila, L.V. Polymerization shrinkage of experimental short glass fiber-reinforced composite with semi-inter penetrating polymer network matrix. *Dent. Mater.* **2008**, *24*, 211–215. [[CrossRef](#)] [[PubMed](#)]
4. Yadav, R.; Kumar, M. Dental restorative composite materials: A review. *J. Oral Biosci.* **2019**, *61*, 78–83. [[CrossRef](#)]
5. Lins, R.; Vinagre, A.; Alberto, N.; Domingues, M.F.; Messias, A.; Martins, L.R.; Nogueira, R.; Ramos, J.C. Polymerization Shrinkage Evaluation of Restorative Resin-Based Composites Using Fiber Bragg Grating Sensors. *Polymers* **2019**, *11*, 859. [[CrossRef](#)]
6. Shah, P.K.; Stansbury, J.W. Photopolymerization shrinkage-stress reduction in polymer-based dental restoratives by surface modification of fillers. *Dent. Mater.* **2021**, *37*, 578–587. [[CrossRef](#)] [[PubMed](#)]
7. Ilie, N.; Hickel, R. Investigations on a methacrylate-based flowable composite based on the SDR™ technology. *Dent. Mater.* **2011**, *27*, 348–355. [[CrossRef](#)]
8. Zandinejad, A.; Atai, M.; Pahlevan, A. The effect of ceramic and porous fillers on the mechanical properties of experimental dental composites. *Dent. Mater.* **2006**, *22*, 382–387. [[CrossRef](#)]
9. Lassila, L.; Keulemans, F.; Vallittu, P.K.; Garoushi, S. Characterization of restorative short-fiber reinforced dental composites. *Dent. Mater. J.* **2020**, *39*, 992–999. [[CrossRef](#)]
10. Garoushi, S.; Säilynoja, E.; Vallittu, P.K.; Lassila, L. Physical properties and depth of cure of a new short fiber reinforced composite. *Dent. Mater.* **2013**, *29*, 835–841. [[CrossRef](#)]

11. Yancey, E.; Lien, W.; Nuttall, C.; Brewster, J.; Roberts, H.; Vandewalle, K. Properties of a New Nanofiber Restorative Composite. *Oper. Dent.* **2019**, *44*, 34–41. [[CrossRef](#)]
12. Osiewicz, M.A.; Werner, A.; Roeters, F.J.; Kleverlaan, C.J. Wear of bulk-fill resin composites. *Dent. Mater.* **2022**, *38*, 549–553. [[CrossRef](#)] [[PubMed](#)]
13. Ilie, N.; Kreppel, I.; Durner, J. Effect of radical amplified photopolymerization (RAP) in resin-based composites. *Clin. Oral Investig.* **2014**, *18*, 1081–1088. [[CrossRef](#)] [[PubMed](#)]
14. Özduman, Z.C.; Kazak, M.; Fildisi, M.A.; Özlen, R.H.; Dalkilic, E.; Donmez, N. Effect of Polymerization Time and Home Bleaching Agent on the Microhardness and Surface Roughness of Bulk-Fill Composites: A Scanning Electron Microscopy Study. *Scanning* **2019**, *2019*, 2307305. [[CrossRef](#)]
15. *ISO-Standards 2009*; ISO 4049 Dentistry-Polymer-Based Restorative Materials Geneva. International Organization for Standardization: London, UK, 2009.
16. Askeland, D.R. *The Science and Engineering of Materials*; Springer Science Business Media: New York, NY, USA, 1996; ISBN 978-1-4899-2895-5. [[CrossRef](#)]
17. Borges, B.C.D.; Groninger, A.I.S.; Soares, G.P.; dos Santos-Daroz, C.B.; Ambrosano, G.M.B.; Marchi, G.M.; Giorgi, M.C.C.; Aguiar, F.H.B. Curing Quality of Composites as Influenced by the Filler Content, Light Source and Curing Time. *Dentistry* **2012**, *1*, 103. [[CrossRef](#)]
18. Kim, K.-H.; Ong, J.L.; Okuno, O. The effect of filler loading and morphology on the mechanical properties of contemporary composites. *J. Prosthet. Dent.* **2002**, *87*, 642–649. [[CrossRef](#)]
19. McCabe, J.F.; Wassell, R.W. Hardness of model dental composites—The effect of filler volume fraction and silanation. *J. Mater. Sci. Mater. Med.* **1999**, *10*, 291–294. [[CrossRef](#)]
20. Alshabib, A.; Silikas, N.; Watts, D.C. Hardness and fracture toughness of resin-composite materials with and without fibers. *Dent. Mater.* **2019**, *35*, 1194–1203. [[CrossRef](#)]
21. Wang, R.; Habib, E.; Zhu, X. Evaluation of the filler packing structures in dental resin composites: From theory to practice. *Dent. Mater.* **2018**, *34*, 1014–1023. [[CrossRef](#)] [[PubMed](#)]
22. Uyar, T.; Çökeliler, D.; Doğan, M.; Koçum, I.C.; Karatay, O.; Denkbaş, E.B. Electrospun nanofiber reinforcement of dental composites with electromagnetic alignment approach. *Mater. Sci. Eng. C* **2016**, *62*, 762–770. [[CrossRef](#)]
23. Catelan, A.; Mainardi, M.D.C.A.J.; Soares, G.P.; de Lima, A.F.; Ambrosano, G.M.B.; Lima, D.A.N.L.; Marchi, G.M.; Aguiar, F.H.B. Effect of light curing protocol on degree of conversion of composites. *Acta Odontol. Scand.* **2014**, *72*, 898–902. [[CrossRef](#)] [[PubMed](#)]
24. Heintze, S.D.; Zimmerli, B. Relevance of in vitro tests of adhesive and composite dental materials, a review in 3 parts. Part 1: Approval requirements and standardized testing of composite materials according to ISO specifications. *Schweiz. Monatsschrift Fur Zahnmed.* **2011**, *121*, 804–816.
25. Eweis, A.; Yap, A.; Yahya, N. Comparison of Flexural Properties of Bulk-fill Restorative/Flowable Composites and Their Conventional Counterparts. *Oper. Dent.* **2020**, *45*, 41–51. [[CrossRef](#)] [[PubMed](#)]
26. Chung, S.; Yap, A.U.J.; Chandra, S.P.; Lim, C.T. Flexural Strength of Dental Composite Restoratives: Comparison of Biaxial and Three-Point Bending Test. *J. Biomed. Mater. Res.* **2004**, *71*, 278–283. [[CrossRef](#)]
27. Suzuki, N.; Yamaguchi, S.; Hirose, N.; Tanaka, R.; Takahashi, Y.; Imazato, S.; Hayashi, M. Evaluation of physical properties of fiber-reinforced composite resin. *Dent. Mater.* **2020**, *36*, 987–996. [[CrossRef](#)]
28. Bijelic-Donova Uctasli, S.; Vallittu, P.K.; Lassila, L.V.J. Short fiber based filling composites original and repair bulk fracture resistance of particle filler and short fiber-reinforced composites. *Oper. Dent.* **2018**, *43*, E232–E242. [[CrossRef](#)]
29. Vallittu, P.K. High-aspect ratio fillers: Fiber-reinforced composites and their anisotropic properties. *Dent. Mater.* **2015**, *31*, 1–7. [[CrossRef](#)]
30. Van Ende, A.; De Munck, J.; Van Landuyt, K.L.; Poitevin, A.; Peumans, M.; Van Meerbeek, B. Bulk-filling of high C-factor posterior cavities: Effect on adhesion to cavity-bottom dentin. *Dent. Mater.* **2013**, *29*, 269–277. [[CrossRef](#)]
31. Lee, J.H.; Um, C.M.; Lee, I.B. Rheological properties of resin composites according to variations in monomer and filler composition. *Dent. Mater.* **2006**, *22*, 515–526. [[CrossRef](#)]
32. Oglakci, B.; Halacoglu, D.M.; Özduman, Z.C.; Dalkilic, E.E. Volumetric change and gap formation in class V composite restorations: A micro-CT analysis. *J. Adhes. Sci. Technol.* **2020**, *34*, 2725–2742. [[CrossRef](#)]
33. Correia, A.; Andrade, M.R.; Tribst, J.; Borges, A.; Caneppele, T. Influence of Bulk-fill Restoration on Polymerization Shrinkage Stress and Marginal Gap Formation in Class V Restorations. *Oper. Dent.* **2020**, *45*, E207–E216. [[CrossRef](#)]
34. Shah, P.K.; Stansbury, J.W.; Bowman, C.N. Application of an addition-fragmentation-chain transfer monomer in di(meth)acrylate network formation to reduce polymerization shrinkage stress. *Polym. Chem.* **2017**, *8*, 4339–4351. [[CrossRef](#)] [[PubMed](#)]
35. Alshabib, A.; Jurado, C.A.; Tsujimoto, A. Short fiber-reinforced resin-based composites (SFRCS); Current status and future perspectives. *Dent. Mater. J.* **2022**, *41*, 647–654. [[CrossRef](#)] [[PubMed](#)]
36. Deliperi, S.; Alleman, D.; Rudo, D. Stress-reduced direct composites for the restoration of structurally compromised teeth: Fiber design according to the “wallpapering” technique. *Oper. Dent.* **2017**, *42*, 233–243. [[CrossRef](#)] [[PubMed](#)]
37. Anttila, E.J.; Krintila, O.H.; Laurila, T.K.; Lassila, L.V.; Vallittu, P.K.; Hernberg, R.G. Evaluation of polymerization shrinkage and hydroscopic expansion of fiber-reinforced biocomposites using optical fiber Bragg grating sensors. *Dent. Mater.* **2008**, *24*, 1720–1727. [[CrossRef](#)] [[PubMed](#)]

38. Amirouche-Korichi, A.; Mouzali, M.; Watts, D.C. Effects of monomer ratios and highly radiopaque fillers on degree of conversion and shrinkage-strain of dental resin composites. *Dent. Mater.* **2009**, *25*, 1411–1418. [[CrossRef](#)]
39. Papadogiannis, D.; Tolifid, K.; Gerasimou, P.; Lakes, R.; Papadogiannis, Y. Viscoelastic properties, creep behavior and degree of conversion of bulk fill composite resins. *Dent. Mater.* **2015**, *31*, 1533–1541. [[CrossRef](#)]

Disclaimer/Publisher’s Note: The statements, opinions and data contained in all publications are solely those of the individual author(s) and contributor(s) and not of MDPI and/or the editor(s). MDPI and/or the editor(s) disclaim responsibility for any injury to people or property resulting from any ideas, methods, instructions or products referred to in the content.